Desalination and Water Treatment
www.deswater.com

doi: 10.5004/dwt.2017.20183

63 (2017) 78–86
February

Synthetic textile wastewater treatment: removal of Nylosan (N-2RBL) dye by electrocoagulation

Amel Belayachi-Haddad[a,*], Nouredine Benderdouche[a], Benaouda Bestani[a], Laurent Duclaux[b]

[a]*Laboratoire de :structure, élaboration et application de matériaux moléculaires, SEA2M, Abdelhamid Ibn Badis University, B.P. 227, Mostaganem, 27000, Algeria, Tel. +213(0)790484975; Fax: +213(0)790484975; emails: belamel@live.com (A. Belayachi-Haddad), benderdouchen@yahoo.fr (N. Benderdouche), bestanib@yahoo.fr (B. Bestani)*
[b]*Laboratoire de: chimie moléculaire et environnement, LCME, University of Savoie- Mont Blanc, 73376, le Bourget du Lac Cedex, France, email: laurent.duclaux@univ-savoie.fr*

Received 29 March 2016; Accepted 21 August 2016

ABSTRACT

Textile wastewater removal requires a detailed study of numerous processing steps. The effectiveness of the electrocoagulation process used to remove a dye from wastewater was evaluated in this study. The effect of initial pH, current density, initial dye concentration, electrolyte concentration, inter-electrode distance, stirring speed, and temperature on the treatment efficiency of the N-2RBL Nylosan Red (NR) dye was investigated. Experimental conditions resulting in more than 98% dye colour removal from a 200 μM dye solution at 303 K were obtained at pH 2.5 with a current density of 13.76 mA/cm^2, electrolyte concentration of 4 g/L, electrolysis time of 8 min, inter-electrode distance of 2.5 cm, and stirring speed of 275 rpm. The sludge and NR dye were characterized by FT-IR spectroscopy, which showed broad vibration stretching modes around 3,630 and 2,930 cm^{-1} assigned to hydroxyl groups from basic aluminum hydroxide/oxyhydroxide groups and C-H aliphatic stretching, respectively. Common peaks observed for both dye and sludge spectra show the presence of the dye in the sludge or of a secondary product resulting from dye oxidation. Measurements show that about 57.6 mg/L COD remained in the treated water, corresponding to an acceptable concentration for organic dyes to be discharged in urban sewage or water bodies. This study shows the feasibility of using simple electrocoagulation for textile dye removal.

Keywords: Nylosan Red; Electrocoagulation; Aluminum electrodes; Sludge; Aqueous solution

1. Introduction

The main environmental problem that arises in the textile industry is the amount and chemical composition of discharged water. Often, wastewater has an intense colour, a high pH value, a significant amount of suspended particles, and high chemical oxygen demand. The textile industry uses around 10,000 dye types. Most dyes are toxic with significant environmental and health risks (eutrophication, bioaccumulation, cancer). Around 15% of the dyes used are found in liquid wastewater streams that could end up in rivers and seas [1]. These effluents must be treated before final discharge to avoid environmental and legal consequences.

Conventional methods generally used for the removal of dyes from industrial wastewater consist of biological and physicochemical treatments and their various combinations [2,3]. Biological treatment usually requires low capital cost. However, biological treatments do not always give rise to satisfactory results, particularly in the case of industrial wastewater. This is due to the production of many industrial organic substances that are considered inhibitory, toxic and/or resistant to biological treatments.

* Corresponding author.

Physicochemical methods are generally based on adsorption (using for example activated carbon), coagulation/flocculation (using salts or inorganic polymers), chemical oxidation (chlorination, ozonation, etc.) and photodegradation (UV/H_2O_2, UV/T_iO_2) [4–6]. However, these treatment methods usually require chemicals, which sometimes lead to secondary pollution and a large volume of waste solids [7–9]. There are also alternative methods that do not need chemicals, such as membrane processes. Recently, it has been shown that electrochemical techniques may provide a cost-effective, scalable, and environment-friendly alternative for wastewater treatment [10].

Electrolysis can have direct or indirect effects on dissolved species. Small sized pollutants can be directly oxidised or reduced near the electrodes. This is the case of ions or small molecules, chemicals and colloids. In some cases, anodic oxidation (or cathodic reduction) is ineffective or slow. It is then necessary to generate an oxidant that reacts electrochemically with large molecules, suspended solids and bacteria [11].

The literature shows that the electrocoagulation technique offers simplicity, efficiency, environmental compatibility, safety and selectivity [9,12].

Electrocoagulation (EC) uses soluble anodes. Following current (or potential) application between two electrodes (mostly iron or aluminium) immersed in an electrolyte contained in a reactor, in situ ions (Fe^{2+}, Fe^{3+}, Al^{3+}) generation causes coagulation-flocculation of pollutants. Electrolysis may also coagulate oxidizable or reducible soluble compounds contained in the effluent.

The main reaction that occurs at the aluminium anode is a dissolution reaction [13]:

$$Al_{(s)} \rightarrow Al^{3+} + 3e^- \quad (1)$$

Moreover, electrolysis of water occurs at the cathode and the anode [13]:

$$2H_2O + 2e^- \rightarrow H_{2(g)} + 2OH^- \quad (2)$$

$$2H_2O \rightarrow 4H^+ + O_{2(g)} + 4e^- \quad (3)$$

Interactions between aluminium ions and hydroxide generated at the surface of the electrodes react to give rise to polymeric products [14].

$$Al^{3+} + 3OH^- \rightarrow Al(OH)_{3(s)} \quad (4)$$

$$n\ Al(OH)_{3(s)} \rightarrow Al_n(OH)_{3n(s)} \quad (5)$$

The insoluble aluminium hydroxide with a large surface area [15] can quickly remove the dye molecules by electrostatic attraction or complex bonding at the interface. In the case of these interface interactions, the pollutant can act as a ligand to bind to a fragment of hydrated aluminium by precipitation and adsorption [13].

Depending on the hydroxide structure, the precipitation process could be explained through the following mechanisms:

$$Dye + Monomer\ Al \rightarrow [Dye\text{-}Monomer\ Al]_s \quad (6)$$

$$Dye + Polymer\ Al \rightarrow [Dye\text{-}Polymer\ Al]_s \quad (7)$$

The adsorption may involve one of the two mechanisms described below:

$$Dye + Al(OH)_{n(s)} \rightarrow Sludge \quad (8)$$

$$Dye + [Dye\text{-}Polymer\ Al]_s + Al(OH)_{n(s)} \rightarrow Sludge \quad (9)$$

The aim of this study was to (i): examine the effects of experimental parameters such as initial pH, initial dye concentration, current density, electrolyte concentration, temperature, stirring speed, and inter-electrode distance. (ii): Characterize the sludge from the EC treatment by thermogravimetric analysis and FT-infrared spectroscopy. This parametric study will improve the efficiency and cost effectiveness of the electrocoagulation process. We used a 200 μM NR solution as an artificial wastewater.

2. Materials and methods

2.1. Electrocoagulation experimental setup

The experimental setup of the electrocoagulation process is shown in Fig. 1. A Plexiglas vessel (45 × 20 × 15 cm) and a thermostat allowing temperature control and a 300 mL beaker with an effective volume of 200 mL were used. Two identical aluminium electrodes with the following dimensions were used as anode and cathode: length (L) = 4 cm, width (W) = 1.3 cm, and thickness (t) = 0.1 cm. These two electrodes were immersed in the solution to achieve an active electrode area of 7.27 cm^2 and an inter-electrode distance of 2.5 cm. The electrodes were connected to a stabilised DC power supply (PE 00 1540, 0-3 A, 0-40 V).

2.2. Experimental approach

A 200 mL solution was prepared by dissolving a proper amount of N-2RBL Nylosan Red (NR) dye (Fig. 2) in distilled water to obtain a 200 μM initial concentration. Na_2SO_4 was added to the solution in 0.5 g/L concentration as a support electrolyte to increase the conductivity of the solution and facilitate the electrocoagulation process. The prepared solution was placed in the electrochemical cell and stirred with

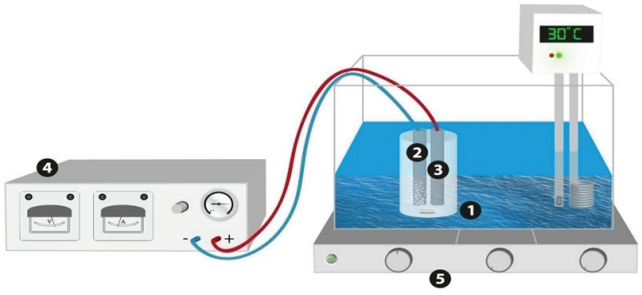

Fig. 1. Schematic representation of the electrocoagulation setup used in this study: 1- electrochemical cell; 2- cathode (Aluminium); 3- anode (Aluminium); 4- DC power supply; 5- magnetic stirring.

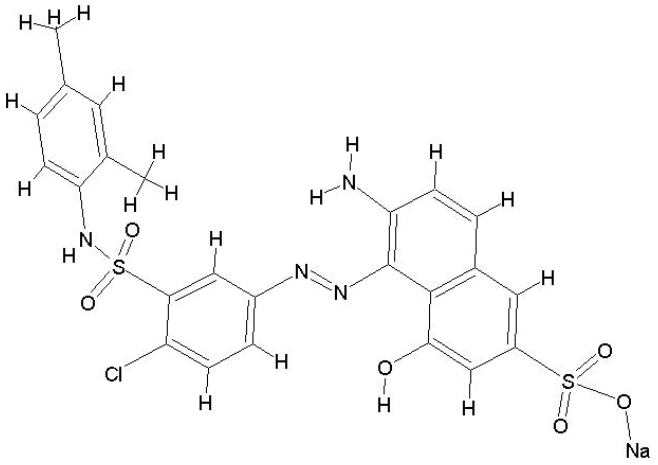

Fig. 2. The molecular structure of Nylosan Red dye.

a magnetic stirrer (SB 161-3 Stuart, Stone, Staffordshire, UK) until the mixture became homogeneous. Electrochemical coagulation experiments were carried out under galvanostatic conditions. Before each experiment, the pH of the solution was adjusted to the desired pH value by using HCl (1 N) and NaOH (0.1 N). pH values were measured using a (HI pH-211, HANNA Instruments, Woonsocket, Rhode Island, USA) pH-meter.

Electrodes were etched in a dilute HCl solution and degreased in a soap solution then rinsed repeatedly with distilled water to remove dirt.

Samples of dye solution were electrolysed at different time intervals and 5 mL were removed from the vessel for analysis using transfer pipettes. The samples were filtered through an ordinary filter paper and then analysed [16–18]. Analyses were performed using a UV-Vis spectrophotometer (Jenway 7305 Spectrophotometer, Staffordshire, UK) to determine the extent of colour removal. Absorbance measurements at λ_{max} = 500 nm were carried out to follow colour change. Chemical oxygen demand (COD) using the open reflux method according to the standard procedure [19] was also used to determine the amount of chemically oxidizable substances in the dye solution.

In Fourier transform infrared spectroscopy, IR radiation is passed through a sample, which absorbs some of the radiation and transmits some of it. The resulting spectrum represents the molecular absorption and transmission creating a fingerprint of the sample. This technique is used to identify unknown materials as the absorption peaks correspond to the frequencies of vibrations between the bonds of the atoms making up the material. The FTIR spectra of formed sludge and NR dye were determined using the pressed disk method with potassium bromide on an irprestige-21 Shimadzu FTIR spectrometer.

The formed sludge and NR dye were characterized by thermogravimetric analysis (TGA) in a homemade apparatus (university of Savoie, France) equipped with a Mettler balance (± 0.1 mg). TGA is a technique that measures the change in weight (weight loss) as the sample is heated, cooled or held at constant temperature. It is used to characterize the sample with regard to its composition. About 200 mg of samples were heated from 25 to 1,000°C at a heating rate of 10°C min^{-1} under nitrogen flow.

The colour change and COD levels were determined using Eqs. (10) and (11), respectively.

$$Y_{Col}(\%) = \frac{A_0 - A}{A_0} \cdot 100 \quad (10)$$

$$Y_{COD}(\%) = \frac{COD_0 - COD}{COD_0} \cdot 100 \quad (11)$$

where A_0 and A are absorbance values before and after electrocoagulation, respectively [13]. The same index "0" was used to distinguish the initial and final *COD* values.

The specific electrical energy consumption per kg of dye removed (kWh/kg) was estimated using Eq. (12).

$$E_{dye} = \frac{U \cdot I \cdot t}{1000 \cdot V \cdot C_0 \cdot Y_{Col}} \quad (12)$$

where C_0 (kg/m^3) is the dye initial concentration, I (A) the current, U (V) the cell voltage, t (h) the electrolysis time, and V (m^3) the volume of liquid.

3. Results and discussion

3.1. Effect of pH

The initial pH is known as one of the main factors affecting the overall performance of electrocoagulation [20,21]. The influence of initial pH on the NR dye removal is depicted in Fig. 3. Maximum decolourization (98.58%) was observed at pH 2.5 after 8 min of electrolysing. The pH value found is in good agreement with those reported elsewhere (2–3 range) [13,22,23], while in this work, the least efficient process was obtained at pH 9.

The pH was found to change during the electrocoagulation process as also reported elsewhere [1,24,25]. The pH increase can be attributed to the higher concentration of hydroxide ions OH^- in the solution, resulting from water reduction at the cathode [26,27] as shown in Eq. (13):

$$2H_2O_{(l)} + 2e^- \rightleftharpoons H_{2(g)} + 2OH^- \quad (13)$$

In addition, the dye and aluminium hydroxide could form complexes through an ionic bond [28,29]. This process also results in a pH increase as follows:

$$R - SO_3Na + (OH)_3(H_2O)Al \rightarrow R - SO_3 - (OH)_2H_2OAl + Na^+ + OH^- \quad (14)$$

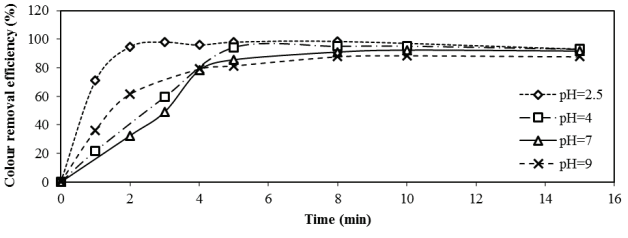

Fig. 3. Effect of pH on the dye removal at different time intervals. [NR] = 200 μM, j = 13.76 mA/cm^2, [Na_2SO_4] = 0.5 g/L, stirring speed = 275 rpm, d = 2.5 cm, T = 303 K.

According to Kobya et al. [22], the decrease of pH versus time in basic solutions (pH ≥ 9) is due to the consumption of OH^- ions by aluminium hydroxide $Al(OH)_{3(s)}$ resulting in $Al(OH)_4^-$ ions.

The aluminium cation dissolved electrochemically at the anode is hydrolysed to form monomers or polymers species according to the following reaction [30]:

$$xAl^{3+} + yH_2O \rightarrow Al_x(OH)^{(3x-y)+} + yH^+ \quad (15)$$

Dominant aluminium species may vary depending on the pH of the solution. Al^{3+} and $Al(OH)^{2+}$ species are dominant at pH 2-3. At pH in the range of 4–9, various polymeric species such as $Al_{13}O_4(OH)_{24}^{7+}$ are formed and lead to $Al(OH)_{3(S)}$ precipitates [22].

A possible explanation for this observation is that the removal efficiency of NR gradually decreases with increasing pH. The wide range of initial optimal pH reported in the literature shows that the removal of dye by EC may result from several complex mechanisms [31].

An alternative explanation may be that at pH 2.5, production of Al^{3+} is sufficient to remove the dye entailing the high removal efficiency. Indeed, the formed EC floc obtained may have a good affinity with the various forms of aluminium ions [32]. In addition, pH may strongly affect adsorption depending on the chemical structure of the adsorbed species.

3.2. Influence of current density

Current density is a critical electrocoagulation parameter. The effect of current density on the removal of the NR dye was studied by varying the current density from 3.44 to 20.63 mA/cm^2. Fig. 4 shows the influence of current density on the removal efficiency of NR.

When the current density increased from 3.44 to 13.76 mA/cm^2, the removal efficiency of NR increased from 97.24% to 98.58%, but when it exceeded 13.76 mA/cm^2, the dye removal efficiency became almost constant. This can be explained by the fact that the amount of aluminium ions passing through the solution increased with current density because of the electrode dissolution according to Faraday's law. This leads to additional destabilisation of the pollutant particles and neutralization of their charges. As a consequence, electrostatic repulsion between particles is reduced to the point where van der Waals attraction will dominate and result in agglomeration. The aluminium hydroxide flocs formed adsorb and remove dye ions from the solution [13,17,33]. Furthermore, the production rate of the hydrogen bubbles increases while these decrease in size with current density. All these effects are beneficial for an effective pollutant removal by flotation [7]. Assessment of the effect electrocoagulation parameters may help improve overall removal efficiency.

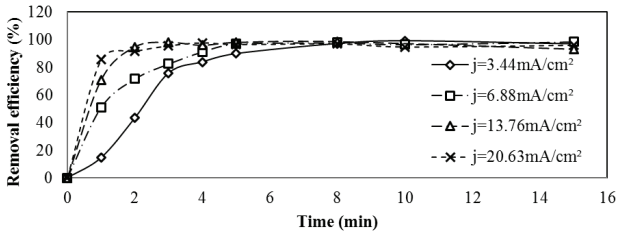

Fig. 4. Effect of current density on dye removal at different time intervals. [NR] = 200 μM, pH = 2.5, [Na_2SO_4] = 0.5 g/L, stirring speed = 275 rpm, d = 2.5 cm, T = 303 K.

Operating at high current densities may give rise to other side reactions in the vicinity of the anode. For example, direct oxidation of the pollutant and formation of oxygen may occur. Oxygen production near the anode indicated in the following reaction (Eq. (16)) will likely reduce the effectiveness of the electrocoagulation process [7]. Table 1 reports some removal efficiency values versus current density.

$$4OH^- \rightarrow O_2 + 2H_2O + 4e^- \quad (16)$$

It can be seen from Fig. 4 and Table 1 that beyond a current density of 13.76 mA/cm^2, the removal efficiency decreased from 98.58% to 97.45%. High current density will also reduce cathode efficiency through the deposition of oxide film [34]. This leads to a high consumption of energy by the Joule effect and increased costs of treatment [35,36]. On the other hand, the slope was positive and equal to +0.26 when the current density varied from 3.44 to 13.76 mA/cm^2. Therefore, the value 13.76 mA/cm^2 was chosen as the appropriate current density for following experiments.

Energy consumption increases drastically with current density as shown in Fig. 5. The present observations agree with previously reported data in the literature for textile industry wastewater [1,31,37]. Hence, electric current density is an important parameter for reducing energy input.

3.3. Influence of the dye concentration

Fig. 6 shows the effect of the initial dye concentration on dye removal efficiency. Except for an initial dye concentration of 700 μM, the removal efficiency increased with time before reaching a plateau. At a high initial concentration (700 μM), the removal efficiency did not change with time. These observations corroborate the data previously reported in the literature [29]. This behaviour has been explained in the past using Faraday's law [13,22,35]. Indeed, for a given current density and electrolysis time, the amount of dissolved aluminium ions in the anode is constant for all dye concentrations. A constant number of complex aluminium hydroxide species is thus formed in the solution. Therefore, the produced flocs are insufficient to adsorb a large number of the dye molecules.

Table 1
Effect of current density on removal efficiency

j (mA/cm^2)	Removal efficiency (%)
3.44	97.24 ± 0.13
6.88	97.91 ± 0.11
13.76	98.58 ± 0.07
20.63	97.45 ± 0.12

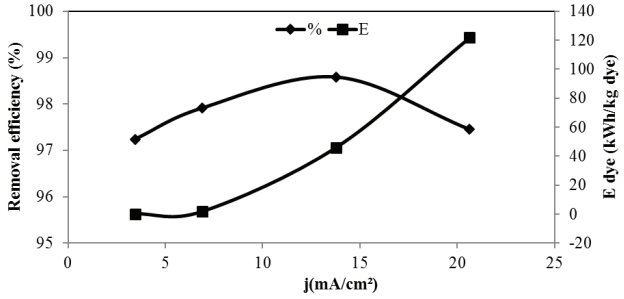

Fig. 5. Influence of current density on the removal efficiency of NR and the specific energy consumption. [NR] = 200 μM, pH = 2.5, [Na_2SO_4] = 0.5 g/L, stirring speed = 275 rpm, d = 2.5 cm, T = 303 K, t = 8 min.

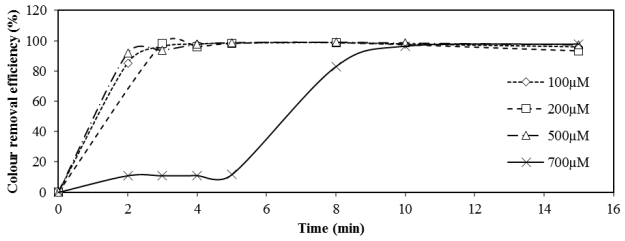

Fig. 6. Effect of dye concentration on the dye removal at different time intervals. pH = 2.5, [Na_2SO_4] = 0.5 g/L, j = 13.76 mA/cm^2, stirring speed = 275 rpm, d = 2.5 cm, T = 303 K.

3.4. Influence of conductivity

Concentration of sodium sulphate was varied to study the impact of the conductivity of the solution on the efficiency of electrocoagulation. According to several authors [9,30], the increase in conductivity reduces the voltage U between the electrodes for a given constant current density. This was attributed to the decrease in the resistance of the polluted water. Thus, energy consumption, which is proportional to the voltage applied between the electrodes, is expected to decrease.

Conductivity of the solution depends on the number of ions present. Increasing the electrolyte concentration leads to an increase in the number of ions. The solution eventually becomes more conductive, which results in increased current density within the medium. This will lead to higher removal efficiency [33,38]. To determine the effect of conductivity on the colour change, different amounts of sodium sulphate (Na_2SO_4) were added to the starting solution. This electrolyte allows adjusting the conductivity. The results are shown in Fig. 7. Note that the removal efficiency of the NR dye increased with sodium sulphate concentration. Beyond the critical Na_2SO_4 concentration of 4 g/L, the removal efficiency decreases slightly. Decolourization is thus reduced attributed to a change in the ionic strength due to the change in the conductivity of the medium [22]. The ionic strength affects the kinetics and equilibrium reactions involving the different components during the EC process. Typical reactions occurring during the EC are given in Eqs. (17) and (18).

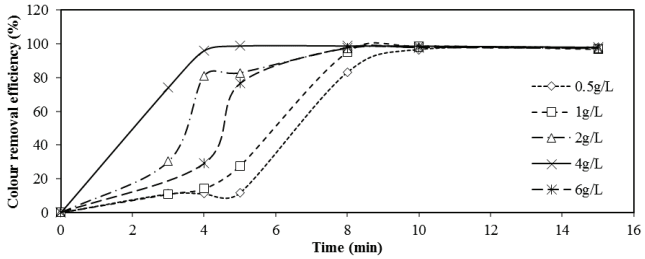

Fig. 7. Influence of the electrolyte concentration on the dye removal at different time intervals. [NR] = 700 μM, pH = 2.5, j = 13.76 mA/cm^2, stirring speed = 275 rpm, d = 2.5 cm, T= 303 K.

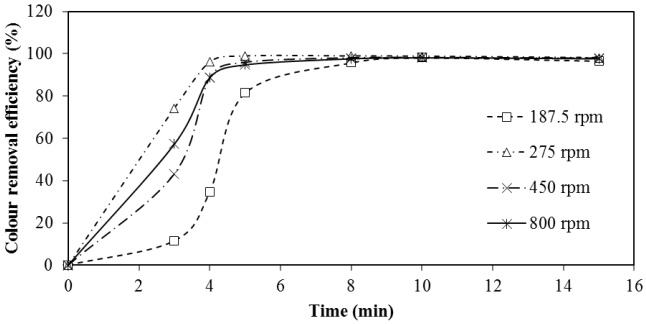

Fig. 8. Influence of the stirring speed on the dye removal at different time intervals. [NR] = 700 μM, pH = 2.5, j = 13.76 mA/cm^2, [Na_2SO_4] = 4 g/L, d = 2.5 cm, T = 303 K.

$$Al^{3+}_{aq} + 3H_2O_{(1)} \rightarrow Al(OH)_{3(s)} + 3H^+_{(aq)} \quad (17)$$

$$Al(OH)_3 + OH^- \rightarrow Al(OH)_4^- \quad (18)$$

3.5. Influence of stirring speed

The stirring speed of the solution increases contact between flocs and corresponding agglomeration particles. However, intense agitation can cause the destruction of flocs. Thus, stirring speed control is important. The influence of stirring speed on dye removal is shown in Fig. 8. Highest dye removal was achieved using a stirring speed of 275 rpm, effecting the conglomeration of flocs and contact with the NR molecules. It can be observed that a speed greater than 275 rpm was not required [19,39].

3.6. Influence of inter-electrode distance

The influence of inter-electrode distance was studied to determine the gap influence on dye removal efficiency. The electrostatic field, which depends on the inter-electrode distance, decreases with inter-electrode distance. The movement of solution ions slows down during electrolysis because of the low electric fields. This facilitates flocculation and linkage between the NR molecules and aluminium hydroxides [38]. The inter-electrode distance should not be

too high to prevent floc formation. As observed in Fig. 9 at 2.5 cm inter-electrode distance, the NR removal efficiency attained its maximum (98.91% after 8 min treatment time). The 2.5 cm inter-electrode distance was used for carrying out the EC process.

3.7. Effect of temperature

The effect of temperature on the electrocoagulation efficiency was rarely investigated [33]. In this work, the influence of temperature on the removal efficiency of the NR dye by EC was also studied. The results are shown in Fig. 10. Removal efficiency was found to decrease with temperature from 303 to 313 K. Similar results were found in the literature [25,33,40]. At high temperatures, the movement of generated ions increases dramatically and therefore the ions have a low probability to coalesce and to produce aluminium hydroxides flocs. High temperatures also cause the formation of undesirable flocs and/or the increase of the solubility of the precipitates [33]. However, at 333 K, the removal efficiency was higher than at 313 K, therefore, the effect of temperature was not conclusive as also observed by Wei-Lung Chou and Phalakornkule et al. [26,33].

3.8. UV-visible spectrum of the NR dye

The UV-Visible absorption spectra of the dye NR were studied at different times of the electrocoagulation process. The results are shown in Fig. 11. The spectrum of the NR solution has a large band in the visible range, located around 500 nm related to the azo bond and an absorption band in the UV region attributed to the presence of aromatic rings. The peak at 310 nm can be assigned to the cycles of naphthalene. The peak at 230 nm corresponds to the benzene ring [41]. After treatment by the EC process, the band at 500 nm, characteristic of the chromophore group tends to decrease with treatment time. This peak disappeared after 8 min of EC treatment time indicating that the NR dye structure was almost eliminated.

3.9. Comparison between COD and decolourization

The COD value characterizes the amount of chemically oxidizable substances in water. It is the amount of oxygen required to oxidize aqueous organic compounds. The dye removal efficiency (Eq. (10)) and COD abatement (Eq. (11)) are shown in Fig. 12. It is expected that during EC, the removal efficiency and COD abatement would follow the same trend. However, this was not observed in our case as Fig. 12 shows that COD abatement was lower than dye removal efficiency. Similar results were found in the literature [26]. This may be a sign of an electrochemical oxidation of a fraction of the dye in conjunction with its removal during the EC process. Electrochemical oxidation may break the azo dye with no effect on the degradation of aromatic rings [19], which means that a fraction of the pollutant or some electrocoagulation by-products remains in the water after EC. For a 200 μM dye concentration, this corresponds to 80 μM (57.6 mg/L) dye concentration that can be taken as an admissible effluent concentration. The maximum admissible concentration in terms of COD as quality indicator for textile organic dyes discharged in urban sewage network is 500 and 125 mg/L for their direct discharge in water bodies [42].

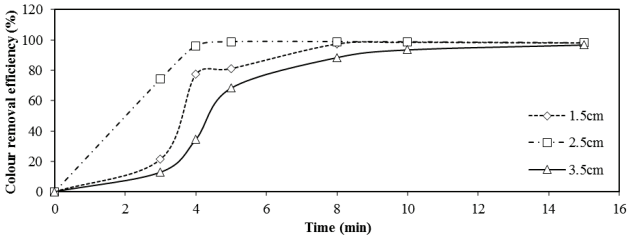

Fig. 9. Influence of the distance between electrodes on the dye removal at different time intervals. [NR] = 700 μM, pH = 2.5, j = 13.76 mA/cm^2, [Na_2SO_4] = 4 g/L, stirring speed = 275 rpm, T = 303 K.

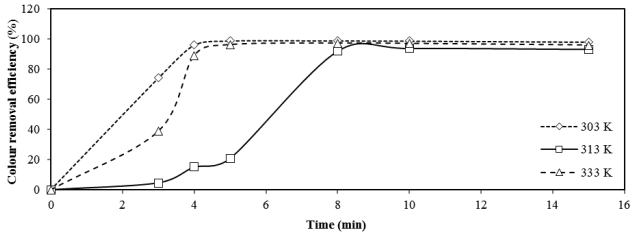

Fig. 10. Influence of temperature on the dye removal at different time intervals. [NR] = 700 μM, pH = 2.5, j = 13.76 mA/cm^2, [Na_2SO_4] = 4 g/L, stirring speed = 275 rpm, e = 2.5 cm.

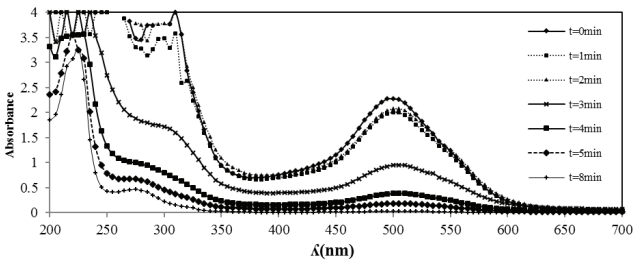

Fig. 11. UV-Vis spectrum of the NR dye at different times of the EC. [NR] = 500 μM, pH = 2.5, j = 13.76 mA/cm^2, [Na_2SO_4] = 4 g/L, stirring speed = 275 rpm, e = 2.5 cm, T = 303 K.

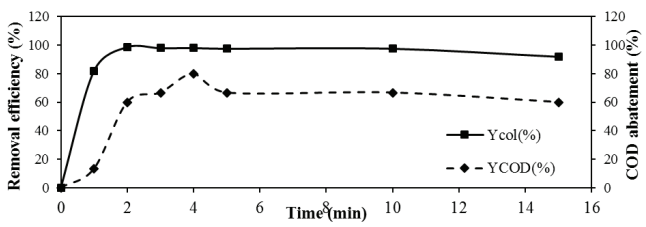

Fig. 12. Variation of dye removal and COD abatement as a function of time. [NR] = 200 μM, pH = 2.5, j = 13.76 mA/cm^2, [Na_2SO_4] = 0.5 g/L, stirring speed = 275 rpm, e = 2.5 cm, T = 303 K.

3.10. Evolution of sludge

In order to minimize energy consumption and sludge production, experiments were carried out to evaluate the different operating times (5, 10, 15, 20, 30, 40, 50 and 60 min). The initial dye concentration and the current density in these trials were 200 μM and 13.76 mA/cm^2, respectively. Fig. 13 shows the dye removal efficiency and the amount of sludge as a function of operating time. Dye removal efficiency increased rapidly during the first minutes of treatment. Only a slight increase in the dye removal was observed before a plateau was reached. The sludge mass increase was different. The amount of sludge increased with operating time even when the dye was almost completely eliminated. Indeed, as the current passes through the electrodes, the production of $Al(OH)_3$ contributes to sludge formation. This process needs improvement to reduce sludge formation.

3.11. Cost of treatment

The estimated cost of treatment by the EC process consists mainly of energy (electricity) consumption cost, materials (electrodes) and other costs such as labour and disposal of sludge [43]. In this paper, only energy and electrode consumption costs were taken into account to estimate the treatment cost.

The treatment cost of 200 mL of water polluted by NR dye under the operating conditions found in the current work was calculated as follows [43]: First, the power consumption was estimated using Eq. (19).

$$P = \text{Watt} = V \times A \tag{19}$$

where V is the applied voltage and A is applied intensity. Replacing V with 8 and A with 0.1, Eq. (20) was obtained.

$$Watt = 8V \times 0.1A = 0.8W \tag{20}$$

Operating time was set at $t = 8\ min$, so energy consumption is (Eq. (21)):

$$E = P \times t = (0.8W \times 8h)/(60 \times 1000) = 1.06 \times 10^{-4}\ kWh \tag{21}$$

The average cost of one kWh is 0.15 USD. The cost of aluminium electrodes is 1.5 USD/kg. The total cost of NR dye treatment was estimated to be: 0.113 USD/m^3.

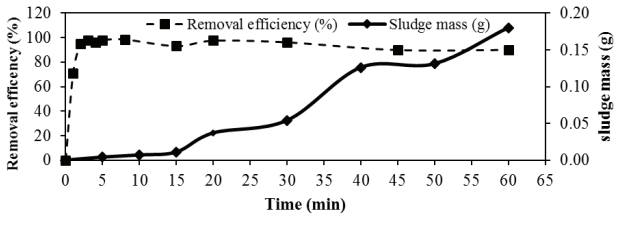

Fig. 13. Variation of dye removal and sludge mass as a function of time. [NR] = 200 μM, pH = 2.5, j = 13.76 mA/cm^2, [Na_2SO_4] = 0.5 g/L, stirring speed = 275 rpm, e = 2.5 cm, T = 303 K.

3.12. Characterization of formed sludge

3.12.1. Thermogravimetric analysis (TGA)

Fig. 14 shows the mass loss evolution of the NR dye and sludge produced after 10 min of treatment by EC as a function of temperature. Measurements were taken from 25 to 1,000°C using a scanning rate of 4°C/min.

At 620°C, the observed 70% mass loss during heat treatment may mainly be due to the electrocoagulated dye fraction in the sludge or to water loss due to hydroxide to oxide conversion. This significant mass loss of the sludge corroborates the removal efficiency as well as the COD reduction values obtained.

3.12.2. FT-IR characterization

The FT-IR spectra of NR dye and the solid by-products using aluminium electrodes resulting from NR electrocoagulation are depicted in Fig. 15.

It can be observed that spectrum (a) shows NH_2 and hydroxyl groups stretching vibrations at 3,338–3,499 cm^{-1} while spectrum (b) shows overlapped peak with broad

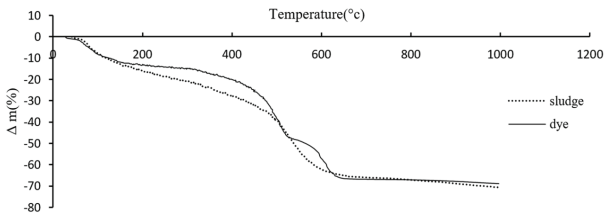

Fig. 14. TGA thermogram of the NR dye and sludge.

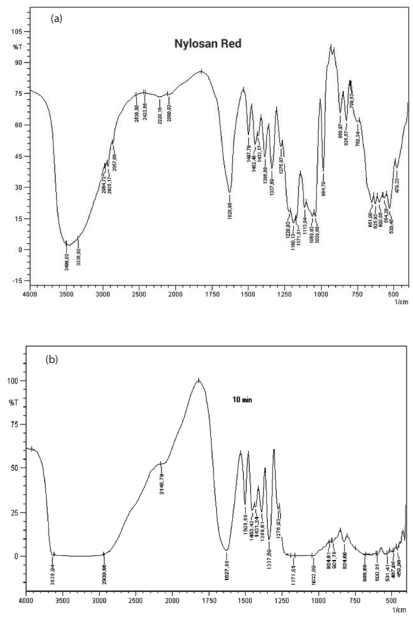

Fig. 15. FT-IR spectra of: (a) NR dye, (b) solid by-products using EC with Al electrodes.

stretching at 2,930–3,630 cm^{-1}, also characteristic of C-H aliphatic stretching and hydroxyl stretching from basic aluminum hydroxide/oxyhydroxide groups. Both spectra show relatively similar peaks characterizing the NR dye. Peaks around 1,172 and 1,338 cm^{-1} can be ascribed to sulfonamide groups (R-SO_2-NR'R''), while the peak around 1,628 cm^{-1} to carbon-carbon double bond stretching.

4. Conclusion

The results of this study clearly demonstrated the viability of the aluminum EC process as a technique for treating efficiently a solution containing Nylosan Red dye. Dye removal efficiency was found to depend on initial pH, current density, dye concentration, electrolyte concentration, inter-electrode distance, stirring speed and temperature. For an initial dye concentration of 200 μM, more than 98% of the dye colour was removed for the following experimental conditions: 8 minutes electrolyzing time, 2.5 initial pH, 13.76 mA/cm^2 current density, 4 g/L sodium sulfate electrolyte concentration, 2.5 cm inter-electrode distance, 275 rpm stirring speed, and 303 K temperature. COD abatement values and sludge thermogravimetric analysis obtained after 10 min treatment time confirmed the efficiency of the EC process. The EC experimental setup for the treatment of synthetic Nylosan Red solutions is simple and cost effective that can be scaled up. Future work will aim at comparing electrocoagulation dye removal efficiency to activated carbon adsorption.

References

[1] N. Daneshvar, A. Oladegaragaze, N. Djafarzadeh, Decolorization of basic dye solutions by electrocoagulation: an investigation of the effect of operational parameters, J. Hazard. Mater., 129 (2006) 116–122.

[2] Y.M. Slokar, A.M. Le Marechal, Methods of decoloration of textilewastewaters, Dyes Pigments, 37 (1998) 335–356.

[3] A.J. Greaves, D.A.S. Phillips, J.A. Taylor, Correlation between the bioelimination of anionic dyes by an activated sewage sludge with molecular structure. Part 1: literature review, Color Technol., 115 (1999) 363–365.

[4] B. Zielinska, J. Grzechuslka, A.W. Morawski, Photocatalytic decomposition of textile dyes on TiO_2-Tytanpol A11 and TiO_2-Degussa P25, J. Photochem. Photobiol. A, 157 (2003) 65–70.

[5] M.V.B. Zanoni, J. Sene, M.A. Anderson, Photoelectrocatalytic degradation of Remazol Brilliant Orange 3R on titanium dioxide thin-film electrodes, J. Photochem. Photobiol. A, 157 (2003) 55–63.

[6] M. Pérez, F. Torrades, X. Doménech, J. Peral, Fenton and photo-Fenton oxidation of textile effluents, Water Res., 36 (2002) 2703–2710.

[7] M. Bennajah, Treatment of Liquid Industrial Waste by Electrocoagulation / Electroflotation in Airlift Reactor, PhD Thesis, National Polytechnic Institute of Toulouse, Toulouse, France, 2007.

[8] T.H. Kim, C. Park, E.-B. Shin, S. Kim, Decolorization of disperse and reactive dyes by continuous electrocoagulation process, Desalination, 150 (2002) 165–175.

[9] M. Bayramoglu, M. Kobya, O.T. Can, M. Sozbir, Operating cost analysis of electrocoagulation of textile dye wastewater, Sep. Purif. Technol., 37 (2004) 117–125.

[10] Marc-Andre Bureau, Stabilization and Electrochemical Treatment of Municipal and Industrial Sludge Purification, Quebec University, Quebec, Canada, 2004.

[11] F. Persin, M. Rumeau, The electrochemical treatment of water and effluent, Water Bull., 42, (1989) 45–56.

[12] M.Y.A. Mollah, S.R. Pathak, P.K. Patil, M. Vayuvegula, T.S. Agrawal, J.A.G. Gomes, M. Kesmez, D.L. Cocke, Treatment of orange II azo-dye by electrocoagulation (EC) technique in a continuous flowcell using sacrificial iron electrodes, J. Hazard. Mater., 109 (2004) 165–171.

[13] E. Pajootan, M. Arami, N. Mohammad Mahmood, Binary system dye removal by electrocoagulation from synthetic and real colored wastewater, J. Taiwan Inst. Chem Eng., 43 (2012) 282–290.

[14] I. Heidmann, W. Calmano, Removal of Zn(II), Cu(II), Ni(II), Ag(I) and Cr(VI) present in aqueous solutions by aluminium electrocoagulation, J Hazard Mater., 152 (2008) 934–941.

[15] S. Farhadi, B. Aminzadeh, V. Khatibikamal, M.A. Fard, Comparison of COD removal from pharmaceutical wastewater by electrocoagulation, photoelectrocoagulation, peroxi-electrocoagulation and peroxi-photoelectrocoagulation processes, J. Hazard. Mater., 219–220 (2012) 35–42.

[16] W.L. Chou, C.T. Wang, K.Y. Huang, Investigation of process parameters for the removal of polyvinyl alcohol from aqueous solution by iron electrocoagulation, Desalination, 251 (2010) 12–19.

[17] F. Akbal, S. Camci, Copper, chromium and nickel removal from metal plating wastewater by electrocoagulation, Desalination, 269 (2011) 214–222.

[18] M.S. Secula, B. Cagnon, T.F. Oliveira, O. Chedeville, H. Fauduet, Removal of acid dye from aqueous solutions by electrocoagulation/GAC adsorption coupling: kinetics and electrical operating costs, J. Taiwan Inst. Chem. Eng., 43 (2012) 767–775.

[19] J.B. Parsa, H.R. Vahidian, A.R. Soleymani, M. Abbasi, Removal of Acid Brown 14 in aqueous media by electrocoagulation: optimization parameters and minimizing of energy consumption, Desalination, 278 (2011) 295–302.

[20] I.A.S. Engil, M. Ozacar, Treatment of dairy wastewaters by electrocoagulation using mild steel electrodes, J. Hazard. Mater. B, 137 (2006) 1197–1205.

[21] X.M. Chen, G.H. Chen, P.L. Yue, Investigation on the electrolysis voltage of electrocoagulation, Chem. Eng. Sci., 57 (2002) 2449–2455.

[22] M. Kobya, E. Demirbas, O.T. Cana, M. Bayramoglu, Treatment of levafix orange textile dye solution by electrocoagulation, J. Hazard. Mater., B132 (2006) 183–188.

[23] J. Zhu, F. Wu, X. Pan, J. Guo, D. Wen, Removal of antimony from antimony mine flotation wastewater by electrocoagulation with aluminum electrodes, J. Environ. Sci., 23 (2011) 1066–1071.

[24] M. Bayramoglu, M. Eyvaz, M. Kobya, Treatment of the textile wastewater by electrocoagulation: economical evaluation, Chem. Eng. J., 128 (2007) 155–161.

[25] S. Song, J. Yao, Z. He, J. Qiu, J. Chen, Effect of operational parameters on the decolorization of C.I. Reactive Blue 19 in aqueous solution by ozone-enhanced electrocoagulation, J. Hazard. Mater., 152 (2008) 204–210.

[26] C. Phalakornkule, S. Polgumhang, W. Tongdaung, B. Karakat, T. Nuyut, Electrocoagulation of blue reactive, red disperse and mixed dyes, and application in treating textile effluent, J. Environ. Manage., 91 (2010) 918–926.

[27] P. Drogui, M. Asselin, S.K. Brar, H. Benmoussa, J.-F. Blais, Electrochemical removal of pollutants from agro-industry wastewaters, Sep. Purif. Technol., 61 (2007) 301–310.

[28] S. Nam, P.G. Tratnyek, Reduction of azo dyes with zero-valent iron, Water Res., 34 (2000) 1837–1845.

[29] S. Engil, I.A. Ozacar, The decolorization of C.I. Reactive Black 5 in aqueous solution by electrocoagulation using sacrificial iron electrodes, J. Hazard. Mater., 161 (2009) 1369–1376.

[30] T. Picard, G. Cathalifaud-Feuillade, M. Mazet, C. Vandensteendam, Cathodid dissolution in the electrocoagulation process using aluminium electrodes, J. Environ. Monit., 2 (2000) 77–800.

[31 B. Merzouk, B. Gourich, A. Sekki, K. Madani, C. Vial, M. Barkaoui, Studies on the decolorization of textile dye wastewater by continuous electrocoagulation process, Chem Eng J., 149 (2009) 207–214.

[32] C.P. Nanseu-Njiki, S.R. Tchamango, P.C. Ngom, A. Darchen, E. Ngameni, Mercury (II) removal from water by electrocoagulation using aluminium and iron electrodes, J. Hazard Mater., 168 (2009) 1430–1436.

[33] W-L. Chou, Removal and adsorption characteristics of polyvinyl alcohol from aqueous solutions using electrocoagulation, J. Hazard Mater., 177 (2010) 842–850.
[34] M. Eyvaz, E. Gürbulak, S. Kara, E. Yükse, Chapter 8, Nanotechnology and Nanomaterials "Modern Electrochemical Methods in Nano, Surface and Corrosion Science", 2014.
[35] A. Erdem Yılmaza, R. Boncukcuoğlua, M. Muhtar Kocaker¥mb, E. Kocadağistana, An empirical model for kinetics of boron removal from boroncontaining wastewaters by the electrocoagulation method in a batch reactor, Desalination, 230 (2008) 288–297.
[36] M. Eyvaz, E. Gürbulak, S. Kara, E. Yüksel, Preventing of Cathode Passivation/Deposition in Electrochemical Treatment methods - A Case Study on Winery wastewater with Electrocoagulation, Modern Electrochemical Methods in Nano, Surface and Corrosion Science, 2014, pp. 201–238.
[37] B. Merzouk, M. Yakoubi, I. Zongo, J-P. Leclerc, G. Paternotte, S. Pontvianne, F. Lapicque, Effect of modification of textile wastewater composition on electrocoagulation efficiency, Desalination, 275 (2011) 181–186.
[38] Z.V.P. Murthy, S. Parmar, Removal of strontium by electrocoagulation using stainless Steel and aluminum electrodes, Desalination, 282 (2011) 63–67.
[39] M. Chi Wei, K. Sung Wang, C. Lin Huang, C. Wei Chaiang, T. Jen Chang, S. Shinn Lee, S. Hsien Chang, Improvement of textile dye removal by electrocoagulation with low-cost steel wool cathode reactor, Chem Eng J., 192 (2012) 37–44.
[40] W-L. Chou, Y-H. Huang, Electrochemical removal of indium ions from aqueous solution using iron electrodes, J. Hazard. Mater., 172 (2009) 46–53.
[41] M. Yousuf, A. Mollah, A. Jewel, G. Gomes, K.K. Das, D.L. Cocke, Electrochemical treatment of Orang II dye solution- Use of aluminium sacrificial electrodes and floc characterization, J. Hazard. Mater., 174 (2010) 851–858.
[42] C. Zaharia, Legislation for Environmental Protection, POLITEHNIUM Ed., ISBN 978-973-621-219-2, Iasi, Romania, 2008.
[43] M. Tejocote-Perez, P. Balderas-Hernandez, C.E. Barrera-Diaz, G. Roa-Morales, R. Natividad-Rangel, Treatment of industrial effluents by a continuous system: electrocoagulation - Activated sludge, Biores. Technol., 101 (2010) 7761–7766.